



## **Technical note: Quantification of flow field variability using intrinsic random function theory**

**Ching-Min Chang<sup>1</sup>, Chuen-Fa Ni<sup>1</sup>, Chi-Ping Lin<sup>2</sup>, and I-Hsian Lee<sup>2</sup>**

<sup>1</sup>Graduate Institute of Applied Geology, National Central University, Taoyuan, Taiwan

<sup>2</sup>Center for Environmental Studies, National Central University, Taoyuan, Taiwan

**Correspondence:** Chuen-Fa Ni ([nichuenfa@geo.ncu.edu.tw](mailto:nichuenfa@geo.ncu.edu.tw))



1    **Abstract.** Much of the stochastic analysis of flow field variability in heterogeneous  
2    aquifers in the literature assumes that the parameters in the associated stochastic flow  
3    equation are weakly (second order) stationary. On this basis, the spectral  
4    representation approach can then be used to quantify the variability of the flow fields  
5    given known covariance functions of the input parameters. However, the condition of  
6    second-order stationarity is rarely encountered in nature and is difficult to verify using  
7    the limited experimental data available. The purpose (or novelty) of this work,  
8    therefore, is to develop a new framework for modeling the variability of the flow  
9    fields that generalizes the stochastic theory that applies to stationary second-order  
10   random input parameters to intrinsic (nonstationary) random input parameters. In this  
11   work, the log hydraulic conductivity and log aquifer thickness are assumed to be  
12   intrinsic random functions for flow through heterogeneous confined aquifers of  
13   variable thickness. On this basis, semivariograms of depth-averaged hydraulic head  
14   and integrated specific discharge fields are developed to characterize the variability of  
15   flow fields. The application of the proposed stochastic theory to the case where the  
16   variability of a random input parameter can be characterized by a linear  
17   semivariogram model is provided.

18

## 19    **1 Introduction**



20

21 Much of the literature on solving the stochastic groundwater flow problem  
22 assumes that the covariance functions of the random input parameters in the  
23 corresponding stochastic differential equation for groundwater flow can be  
24 characterized by spatial covariance functions. Based on these known covariance  
25 functions of parameters, the variability of flow fields in heterogeneous aquifers  
26 can then be represented by the covariances of hydraulic head and specific  
27 discharge using the spectral representation approach (e.g., Dagan, 1989; Gelhar,  
28 1993; Zhang, 2002; Rubin, 2003). It is important to recognize that the approach  
29 is built on the assumption that the random processes of the input parameters are  
30 second order stationary, so they can be represented by a covariance function.  
31 The question arises: can the statistics of the flow field be determined if it is not  
32 possible to identify the covariance function of the input parameter from the  
33 available data or if the covariance functions of the parameter do not exist?

34 In many practical applications, the experimental variance of a random variable  
35 (function) sampled from a field increases with the size of the field (e.g., Desbarats and  
36 Bachu, 1994; Molz et al., 2004; Dell'Oca et al., 2020). This means that the data have an  
37 almost unlimited scattering capacity and cannot be properly described by ascribing a  
38 finite a priori variance to them. This implies that the second-order stationarity



39 hypothesis does not appear to be suitable and that the approach assuming spatial  
40 variation of input parameters characterized by a spatial covariance function in the  
41 treatment of stochastic models of groundwater flow is not appropriate.

42 But even if there is no finite a priori variance, the spatial increments of a random  
43 function may still have a finite variance. Note that the random function that obeys the  
44 intrinsic hypothesis (Matheron, 1965, 1971), i.e., the assumption that the increments of  
45 the random function are weakly stationary, is called the intrinsic (nonstationary) random  
46 function. In this case, the variability of a nonstationary random function can be  
47 characterized by its semivariogram. This implies that it might be possible to determine  
48 the characteristics of the random flow fields based on the known semivariogram of  
49 the random input parameter from the field data for the case of a nonstationary process  
50 of the input parameter. It is clear that the intrinsic hypothesis is weaker than the  
51 second-order stationarity hypothesis.

52 According to Yaglom (1987) and Christakos (1992), an intrinsic function and  
53 its semivariogram admit a spectral representation. From these spectral  
54 representations, the associated stochastic groundwater flow equation can be  
55 solved in the wavenumber domain. Therefore, a spectral relationship between the  
56 wavenumber spectra of the input parameter fluctuations and the spectra of the  
57 output fluctuations can be obtained based on the solution of the stochastic



58 equation. This means that, given intrinsic semivariograms of the input parameters,  
59 the variability of the flow fields can be characterized by the semivariograms of  
60 the hydraulic head and the specific discharge fields using the spectral  
61 representation approach. In other words, it is possible to establish stochastic  
62 theories to characterize the variability of the flow fields without considering the  
63 hypothesis of second-order stationarity for the random input parameters, which is  
64 the goal of this study.

65 This work develops a general stochastic framework for quantifying the variability  
66 of flow fields by semivariograms of depth-averaged hydraulic head and integrated  
67 specific discharge for essentially horizontal steady groundwater flow through a  
68 heterogeneous confined aquifer of variable thickness. It is assumed that the random  
69 input parameters appearing in the associated stochastic differential equation, such as  
70 the log hydraulic conductivity and the log thickness of the confined aquifer, are  
71 intrinsic random functions and therefore nonstationarity in the depth-averaged head  
72 and integrated discharge. This work shows how to develop a stochastic modeling  
73 framework for quantifying the variability of the flow fields given semivariograms of  
74 the random input parameters, which, to our knowledge, has not been presented in the  
75 literature before. An application of the proposed stochastic theories to the case where  
76 the variability of a random input parameter can be characterized by a linear



77 semivariogram model is given.

78

## 79 **2 Statement of the problem**

80

81 In many practical situations, a variable measured on small samples over very short  
82 distances may exhibit very large variations over those distances. To get around this  
83 phenomenon, a variable is often measured as an average over a given volume or area  
84 rather than at a point. This means that in reality the field data are never collected at a  
85 single point, but always include support with finite dimensions, so that the  
86 semivariogram over the sample support can no longer be considered a point  
87 semivariogram (the theoretical semivariogram). Note that the theoretical  
88 semivariogram  $\gamma(\mathbf{h})$  defined at point  $\mathbf{x}$  associated with a pointwise support can be  
89 defined as

$$90 \quad \gamma(\xi) = \frac{1}{2} \text{Var}[Z(\mathbf{x} + \xi) - Z(\mathbf{x})], \quad (1)$$

91 In Eq. (1),  $Z(\mathbf{x})$  is a random function.

92 It can be shown that the semivariogram of an intrinsic random function within a  
93 volume  $\mathcal{V}$  is related to the point-theoretical semivariogram by the formula (e.g.,  
94 Matheron, 1971; Journel and Huijbregts, 1978):

$$95 \quad \gamma_{\mathcal{V}}(\xi) = \frac{1}{\mathcal{V}^2} \int_{\mathcal{V}} \int_{\mathcal{V}} \gamma(\xi + \mathbf{x} - \mathbf{x}') d\mathbf{x}' - \frac{1}{\mathcal{V}^2} \int_{\mathcal{V}} \int_{\mathcal{V}} \gamma(\mathbf{x} - \mathbf{x}') d\mathbf{x}', \quad (2)$$



96 where  $\gamma_r(\mathbf{x})$  is the transformed semivariogram and  $\gamma(\mathbf{x})$  is the theoretical semivariogram  
97 defined in Eq. (1). Matheron (1971) points out that Eq. (2) holds for any intrinsic  
98 random function, even if the covariance function does not exist.

99 This work presents a stochastic analysis of flow through heterogeneous confined  
100 aquifers of variable thickness (see Appendix A). The variability of the flow results  
101 from the variation of the random input parameters, such as the log hydraulic  
102 conductivity and the log thickness of the confined aquifer. In this work, the log  
103 conductivity and log aquifer thickness are considered as spatially intrinsic random  
104 functions whose semivariogram can be represented by Eq. (2). In addition, the  
105 variation of depth-averaged hydraulic head and integrated specific discharge can be  
106 described by the perturbation equations (A3) and (A4), respectively. The spectral  
107 representation approach is used to develop the semivariograms of depth-averaged  
108 hydraulic head and vertically integrated specific discharge to quantify the variability  
109 of the flow fields.

110

### 111 **3 Theoretical developments of semivariograms of flow fields**

112

113 Given the assumption that  $f$  and  $\beta$  in Eq. (A3) satisfy the intrinsic hypothesis, the intrinsic  
114 random functions  $f$  and  $\beta$  each admit a spectral representation of the form (Yaglom, 1987;



115 Christakos, 1992),

$$116 \quad f(x_1, x_2) = \int_{-\infty}^{\infty} \int_{-\infty}^{\infty} \frac{\exp[i(w_1 x_1 + w_2 x_2)] - 1}{i\sqrt{w_1^2 + w_2^2}} dZ_{Sf}(w_1, w_2), \quad (3a)$$

$$117 \quad \beta(x_1, x_2) = \int_{-\infty}^{\infty} \int_{-\infty}^{\infty} \frac{\exp[i(w_1 x_1 + w_2 x_2)] - 1}{i\sqrt{w_1^2 + w_2^2}} dZ_{S\beta}(w_1, w_2), \quad (3b)$$

118 where the  $w_i$  are the components of the wavenumber vector  $\boldsymbol{w} (= (w_1, w_2))$  and  $Sf(w_1, w_2)$   
119 and  $S\beta(w_1, w_2)$  are stationary spatial random processes with uncorrelated complex  
120 Fourier increments  $dZ_{Sf}(w_1, w_2)$  and  $dZ_{S\beta}(w_1, w_2)$ , respectively. Due to the property of the  
121 linearity of the driving forces in Eq. (A3), the depth-averaged head perturbation can  
122 alternatively be decomposed into two parts as

$$123 \quad h(x_1, x_2) = h_f(x_1, x_2) + h_\beta(x_1, x_2), \quad (4a)$$

124 where  $h_f$  represents the head fluctuation in response to the change in log hydraulic  
125 conductivity, while  $h_\beta$  represents the head fluctuation in response to the change in log  
126 thickness of the aquifer. Without any restrictions, each component of the depth-averaged  
127 head perturbation in Eq. (4a) can be expressed by Fourier-Stieltjes representations  
128 (Priestley, 1965) as follows:

$$129 \quad h_f(x_1, x_2) = \int_{-\infty}^{\infty} \int_{-\infty}^{\infty} A_f(x_1, x_2; w_1, w_2) dZ_{Sf}(w_1, w_2), \quad (4b)$$





$$130 \quad h_{\beta}(x_1, x_2) = \int_{-\infty}^{\infty} \int_{-\infty}^{\infty} A_{\beta}(x_1, x_2; w_1, w_2) dZ_{S\beta}(w_1, w_2). \quad (4c)$$

131 In Eqs. (4b) and (4c),  $A_f$  and  $A_{\beta}$  are referred to as oscillatory functions (Priestley,  
 132 1965).

133 Introducing Eqs. (3)-(4) into Eq. (A3), the solution of Eq. (A3) is

$$134 \quad h_f(x_1, x_2) = J \int_{-\infty}^{\infty} \int_{-\infty}^{\infty} \frac{w_1}{(w_1^2 + w_2^2)^{3/2}} \{1 - \exp[i(w_1 x_1 + w_2 x_2)] + i(w_1 x_1 + w_2 x_2)\} dZ_{Sf}(w_1, w_2), \quad (5a)$$

$$135 \quad h_{\beta}(x_1, x_2) = 2J \int_{-\infty}^{\infty} \int_{-\infty}^{\infty} \frac{w_1}{(w_1^2 + w_2^2)^{3/2}} \{1 - \exp[i(w_1 x_1 + w_2 x_2)] + i(w_1 x_1 + w_2 x_2)\} dZ_{S\beta}(w_1, w_2). \quad (5b)$$

136 That is,

$$137 \quad h(x_1, x_2) = J \int_{-\infty}^{\infty} \int_{-\infty}^{\infty} \frac{w_1}{(w_1^2 + w_2^2)^{3/2}} \{1 - \exp[i(w_1 x_1 + w_2 x_2)] + i(w_1 x_1 + w_2 x_2)\} dZ_{Sf}(w_1, w_2)$$

$$138 \quad + 2J \int_{-\infty}^{\infty} \int_{-\infty}^{\infty} \frac{w_1}{(w_1^2 + w_2^2)^{3/2}} \{1 - \exp[i(w_1 x_1 + w_2 x_2)] + i(w_1 x_1 + w_2 x_2)\} dZ_{S\beta}(w_1, w_2). \quad (5c)$$

139 The details of the development of this solution are given in Appendix B.

140 Furthermore, making use of the spectral representation Eq. (3) and Eq. (5) in Eq.  
 141 (A4), the perturbation for the integrated specific discharge in the direction of  $x_1$  (mean  
 142 flow) is given by

$$143 \quad q_1(x_1, x_2) = q_{f_1}(x_1, x_2) + q_{\beta_1}(x_1, x_2), \quad (6a)$$



144 where

$$145 \quad q_{f_1}(x_1, x_2) = e^{F+B} J \int_{-\infty}^{\infty} \int_{-\infty}^{\infty} \frac{\exp[i(w_1 x_1 + w_2 x_2)] - 1}{i\sqrt{w_1^2 + w_2^2}} \left(1 - \frac{w_1^2}{w^2}\right) dZ_{S_f}(w_1, w_2), \quad (6b)$$

$$146 \quad q_{\beta_1}(x_1, x_2) = e^{F+B} J \int_{-\infty}^{\infty} \int_{-\infty}^{\infty} \frac{\exp[i(w_1 x_1 + w_2 x_2)] - 1}{i\sqrt{w_1^2 + w_2^2}} \left(1 - 2 \frac{w_1^2}{w^2}\right) dZ_{S_\beta}(w_1, w_2). \quad (6c)$$

147 The semivariograms of depth-averaged head can now be calculated using Eq. (5)

148 in Eq. (1)

$$149 \quad \gamma_h(\mathbf{x}, \mathbf{y}) = \gamma_{h_f}(\mathbf{x}, \mathbf{y}) + \gamma_{h_p}(\mathbf{x}, \mathbf{y}), \quad (7a)$$

150 where  $\mathbf{x} = (x_1, x_2)$ ,  $\mathbf{y} = (y_1, y_2)$ , and

$$151 \quad \gamma_{h_f}(\mathbf{x}, \mathbf{y}) = \Xi_1(\mathbf{x} - \mathbf{y}) + r_1 \Xi_2(\mathbf{x}, \mathbf{y}) + r_2 \Xi_3(\mathbf{x}, \mathbf{y}), \quad (7b)$$

$$152 \quad \gamma_{h_p}(\mathbf{x}, \mathbf{y}) = 4[\Omega_1(\mathbf{x} - \mathbf{y}) + r_1 \Omega_2(\mathbf{x}, \mathbf{y}) + r_2 \Omega_3(\mathbf{x}, \mathbf{y})], \quad (7c)$$

153  $r_1 = x_1 - y_1$ ,  $r_2 = x_2 - y_2$ . The expressions for  $\Xi_1$ - $\Xi_3$  and  $\Omega_1$ - $\Omega_3$  in Eq. (7) are given in the

154 Appendix C. Note that the random process of the spectral representation according to

155 Eq. (5) and the semivariogram according to Eq. (7) is called an intrinsic random

156 function of order 1 (Matheron, 1973).

157 Similarly, the application of Eq. (6) in Eq. (1) yields the semivariogram of the

158 integrated specific discharge in the mean flow direction of the form

$$159 \quad \gamma_q(\mathbf{x}, \mathbf{y}) = \gamma_{q_f}(\mathbf{x} - \mathbf{y}) + \gamma_{q_p}(\mathbf{x} - \mathbf{y}), \quad (8a)$$

160 where



$$161 \quad \gamma_{q_f}(\mathbf{x}-\mathbf{y}) = e^{2(F+B)J} \int_{-\infty}^{\infty} \int_{-\infty}^{\infty} \frac{1 - \cos(w_1 r_1) \cos(w_2 r_2)}{w_1^2 + w_2^2} \left(1 - \frac{w_1^2}{w_1^2 + w_2^2}\right)^2 S_{S_f}(w_1, w_2) dw_1 dw_2, \quad (8b)$$

$$162 \quad \gamma_{q_\beta}(\mathbf{x}-\mathbf{y}) = e^{2(F+B)J} \int_{-\infty}^{\infty} \int_{-\infty}^{\infty} \frac{1 - \cos(w_1 r_1) \cos(w_2 r_2)}{w_1^2 + w_2^2} \left(1 - 2 \frac{w_1^2}{w_1^2 + w_2^2}\right)^2 S_{S_\beta}(w_1, w_2) dw_1 dw_2. \quad (8c)$$

163 From Eqs. (6) and (8), it can be seen that the random process for the integrated  
 164 discharge in the mean flow direction is an intrinsic random process (or an intrinsic  
 165 random function of order 0, Matheron, 1973).

166 To evaluate Eqs. (7) and (8), which are used to quantify the variability of flow  
 167 fields, the spectral density functions  $S_{S_f}$  and  $S_{S_\beta}$  must be determined. It can be shown  
 168 that when the intrinsic random function has a spectral representation as in Eq. (3), the  
 169 semivariograms of the intrinsic functions  $f$  and  $\beta$  are related to the covariance  
 170 functions of the stationary processes  $Sf$  and  $S\beta$  by

$$171 \quad \frac{\partial^2}{\partial r_1^2} \gamma_f(\mathbf{x}-\mathbf{y}) + \frac{\partial^2}{\partial r_2^2} \gamma_f(\mathbf{x}-\mathbf{y}) = C_f(\mathbf{x}-\mathbf{y}), \quad (9a)$$

$$172 \quad \frac{\partial^2}{\partial r_1^2} \gamma_\beta(\mathbf{x}-\mathbf{y}) + \frac{\partial^2}{\partial r_2^2} \gamma_\beta(\mathbf{x}-\mathbf{y}) = C_\beta(\mathbf{x}-\mathbf{y}), \quad (9b)$$

173 where  $\gamma_f$  and  $\gamma_\beta$  are semivariograms of  $f$  and  $\beta$  functions, respectively, and  $C_f$  and  $C_\beta$  are  
 174 covariance functions of  $Sf$  and  $S\beta$  processes, respectively. The spectral density functions of  
 175 the fluctuations of  $f$  and  $\beta$  are then obtained by the inverse Fourier transform of  $C_f$  and  
 176  $C_\beta$ , respectively, i.e.,



$$177 \quad S_{S_f}(w_1, w_2) = \frac{1}{(2\pi)^2} \int_{-\infty}^{\infty} \int_{-\infty}^{\infty} \exp[w_1 \xi_1 + w_2 \xi_2] C_f(\xi_1, \xi_2) d\xi_1 d\xi_2, \quad (10a)$$

$$178 \quad S_{S_\beta}(w_1, w_2) = \frac{1}{(2\pi)^2} \int_{-\infty}^{\infty} \int_{-\infty}^{\infty} \exp[w_1 \xi_1 + w_2 \xi_2] C_\beta(\xi_1, \xi_2) d\xi_1 d\xi_2. \quad (10b)$$

179 Equations (7) and (8), together with Eqs. (2), (9), and (10), provide the necessary  
180 framework for quantifying the variability of the flow fields. The results can be  
181 obtained for specific input parameter models. This line of research will be pursued in  
182 the next section.

183

## 184 **4 Application**

185

### 186 **4.1 The linear intrinsic semivariogram**

187

188 If a volume  $\mathcal{V}$  is taken as a straight segment of length  $L$  and the point-theoretical  
189 semivariogram of an input parameter in Eq. (2) is considered to be described by a  
190 linear model (e.g., Journel and Huijbregts, 1978; Bardossy, 1997; Usowicz and Lipiec,  
191 2021), i.e.,

$$192 \quad \gamma(\xi) = \alpha |\xi|, \quad (11)$$

193 then the transformed semivariogram in Eq. (2) can be written as



$$194 \quad \gamma_L(\xi) = \frac{\alpha}{L^2} \int_L^L dx \int_L^L |\xi + x - x'| dx' - \frac{\alpha}{L^2} \int_L^L dx \int_L^L |x - x'| dx' . \quad (12)$$

195 Note that the semivariogram of a second order stationary random function is

196 necessarily bounded, while the semivariogram of an intrinsic random function is not.

197 The integration of Eq. (12) can be performed using the Cauchy algorithm (e.g.,

198 Matheron, 1971)

$$199 \quad \gamma_L(\xi) = \frac{\alpha}{L^2} \int_{-L}^L (L - |x|) |\xi + x| dx - \frac{\alpha}{L^2} \int_{-L}^L (L - |x|) |x| dx$$

$$200 \quad = \alpha \left( |\xi| - \frac{L}{3} \right) \quad |\xi| \geq L. \quad (13)$$

201 The details of this development are given in Appendix D. This result agrees with that

202 of Journel and Huijbregts (1978) obtained by a different integrating approach. Note

203 that  $\gamma_L$  in Eq. (13) reaches  $-L/3$  when  $\xi$  approaches zero, and that this negative value is

204 called the “pseudo-negative nugget effect” (Journel and Huijbregts, 1978) due to

205 regularization.

206 In this study, it is assumed that the variograms of the input parameters depend

207 only on the magnitude of the distance between the two points and not on its direction.

208 The spatial variability of the input parameters (such as the log conductivity and log

209 thickness of the aquifer) can be characterized by the following semivariograms

$$210 \quad \gamma_{L_f}(\xi_1, \xi_2) = \alpha_f \left( |\xi| - \frac{L}{3} \right) \quad |\xi| \geq L, \quad (14a)$$

$$211 \quad \gamma_{L_p}(\xi_1, \xi_2) = \alpha_p \left( |\xi| - \frac{L}{3} \right) \quad |\xi| \geq L, \quad (14b)$$

212 which represent the extension of Eq. (13) to two dimensions. In Eq. (14),  $|\xi| =$



213  $(\xi_1^2 + \xi_2^2)^{1/2}$ .

214 The covariance functions of  $Sf$  and  $S\beta$  processes are determined from substituting Eq.

215 (14) into Eq. (9), respectively,

216 
$$C_f(\xi_1, \xi_2) = \frac{\partial^2}{\partial \xi_1^2} \gamma_{L_f}(\xi_1, \xi_2) + \frac{\partial^2}{\partial \xi_2^2} \gamma_{L_f}(\xi_1, \xi_2) = \frac{\alpha_f}{\sqrt{\xi_1^2 + \xi_2^2}}, \quad (15a)$$

217 
$$C_\beta(\xi_1, \xi_2) = \frac{\partial^2}{\partial \xi_1^2} \gamma_{L_\beta}(\xi_1, \xi_2) + \frac{\partial^2}{\partial \xi_2^2} \gamma_{L_\beta}(\xi_1, \xi_2) = \frac{\alpha_\beta}{\sqrt{\xi_1^2 + \xi_2^2}}. \quad (15b)$$

218 From Eqs. (10) and (15), the corresponding spectral density functions of  $f$  and  $\beta$  are

219 obtained, respectively, as follows:

220 
$$S_{Sf}(w_1, w_2) = \frac{1}{(2\pi)^2} \int_{-\infty}^{\infty} \int_{-\infty}^{\infty} \exp[w_1 \xi_1 + w_2 \xi_2] \frac{\alpha_f}{\sqrt{\xi_1^2 + \xi_2^2}} d\xi_1 d\xi_2 = \frac{\alpha_f}{2\pi} \frac{1}{\sqrt{w_1^2 + w_2^2}}, \quad (16a)$$

221 
$$S_{S\beta}(w_1, w_2) = \frac{1}{(2\pi)^2} \int_{-\infty}^{\infty} \int_{-\infty}^{\infty} \exp[w_1 \xi_1 + w_2 \xi_2] \frac{\alpha_\beta}{\sqrt{\xi_1^2 + \xi_2^2}} d\xi_1 d\xi_2 = \frac{\alpha_\beta}{2\pi} \frac{1}{\sqrt{w_1^2 + w_2^2}}. \quad (16b)$$

222 The semivariogram of depth-averaged hydraulic head used to quantify the

223 variability of the head field can then be obtained by substituting Eq. (16) into Eq. (7)

224 and integrating over the wavenumber range. Note that the first term on the right-hand

225 side of Eq. (7b) or Eq. (7c),  $\Xi_1(\mathbf{x}-\mathbf{y})$  or  $4\Omega(\mathbf{x}-\mathbf{y})$ , is called the generalized covariance

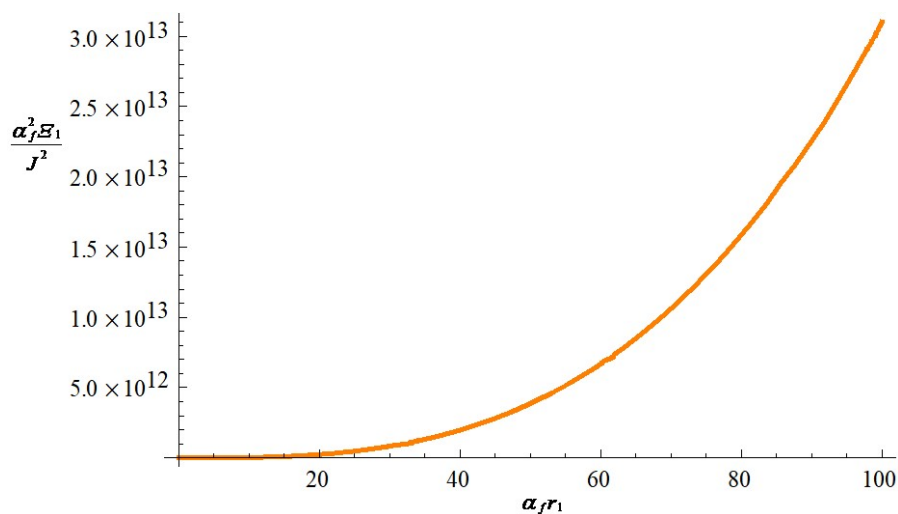
226 function by Matheron (1973). Figure 1 shows the numerical integration result for the

227 generalized covariance function of depth-averaged hydraulic head  $\Xi_1$ , i.e., the

228 component of  $\gamma_{h_f}$  that reflects the effect of variation in hydraulic conductivity fields,



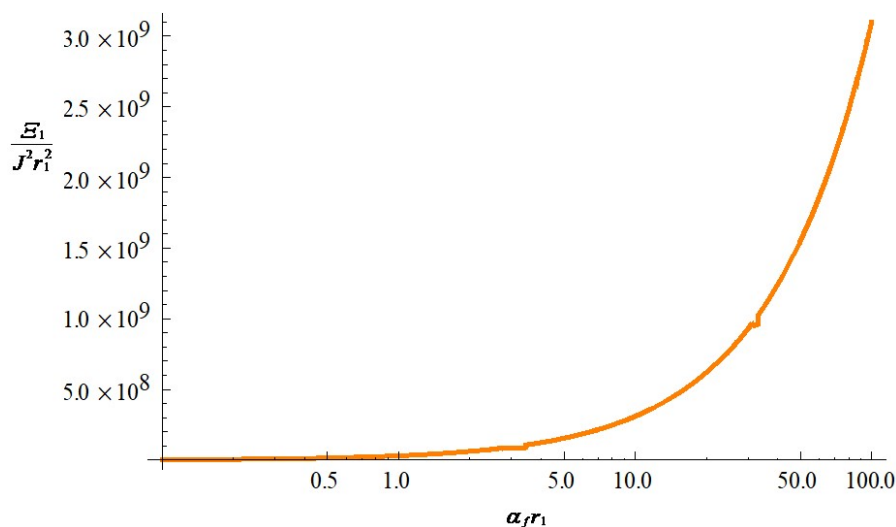
229 using Eq. (16a) in Eq. (C1). The unbounded increase in the generalized covariance  
230 function  $\mathcal{E}_1$  with separation distance suggests that there is no finite depth-averaged head  
231 variance. This implies that the variation in depth-averaged hydraulic head does not  
232 satisfy the second-order stationarity hypothesis. Quantifying the variability in  
233 depth-averaged head using the assumption of second-order stationarity for the input  
234 parameter can lead to a significant underestimation of head variability for the case of  
235 intrinsic random log-conductivity fields. It can also be shown that similar conclusions  
236 can be drawn from the term  $4\Omega_1(\mathbf{x}-\mathbf{y})$  in Eq. (7c), the component of  $\gamma_{h_p}$  reflecting the  
237 effect of variation in the log-aquifer thickness fields, for the case of intrinsic random  
238 log-aquifer thickness fields.



239  
240 **Figure 1.** The generalized covariance function of depth-averaged hydraulic head (the  
241 component of  $\gamma_{h_p}$  that reflects the effect of variation in the log hydraulic conductivity  
242 fields) as a function of separation distance in the mean flow direction, where  $r_1 = x_1 - y_1$ .



243 Figure 2 depicts the behavior of the generalized covariance function  $\Xi_1$  as a  
244 function of parameter  $\alpha_f$  for a given separation distance  $r_1$ . A larger  $\alpha_f$  increases the  
245 variability of the log conductivity fields, resulting in a larger  $\Xi_1$  and thus a larger  
246 semivariogram  $\gamma_h$ . It can also be shown that the larger the parameter  $\alpha_\beta$ , the larger the  
247 variability of the generalized covariance function  $4\Omega_1$ . It can therefore be concluded  
248 that the variability of the depth-averaged hydraulic head caused by the variation of the  
249 log hydraulic conductivity and log aquifer thickness is larger for larger parameters  $\alpha_f$   
250 and  $\alpha_\beta$ .



251  
252 **Figure 2.** The generalized covariance function of depth-averaged hydraulic head (the  
253 component of  $\gamma_h$ , that reflects the effect of variation in the log hydraulic conductivity  
254 fields) as a function of parameter  $\alpha_f$  in the mean flow direction, where  $r_1 = x_1 - y_1$ .

255 The numerical integration results for the components of the semivariogram of the  
256 integrated specific discharge in the mean flow direction,  $\gamma_{q_f}$  and  $\gamma_{q_\beta}$  obtained by





257 substituting Eq. (16) into Eq. (8), are shown in Figs. (3a) and (3b). The unlimited  
258 increase of the integrated discharge semivariogram with the separation distance  
259 shown in Fig. 3 indicates that the variation of the integrated discharge process is  
260 nonstationary. This is the result of the nonstationary process of the depth-averaged  
261 hydraulic head caused by the intrinsic random log-conductivity and log-aquifer  
262 thickness fields. The figure also shows that there is an increase in the semivariogram  
263 of the integrated specific discharge in the mean flow direction with parameters  $\alpha_f$  and  
264  $\alpha_\beta$  for a given separation distance. Larger  $\alpha_f$  and  $\alpha_\beta$  cause greater variability in the  
265 depth-averaged pressure fields and thus greater variability in the integrated specific  
266 discharge fields.

267

## 268 **4.2 The exponential semivariogram**

269

270 It is important to note that the stationary variables always satisfy the intrinsic  
271 hypothesis, while the opposite is not always true, since the intrinsic variable can be  
272 nonstationary. The stochastic theory developed here to quantify the variability of the  
273 flow fields remains valid for any second order stationary random variable. For  
274 example, if the point theoretic semivariogram of an input parameter is chosen as

$$275 \quad \gamma(\xi) = \mu \left( 1 - \exp\left[-\frac{|\xi|}{\lambda}\right] \right), \quad (17)$$



276 the transformed semivariogram over a segment of length  $L$  can then be calculated

277 using Eq. (2) and the Cauchy algorithm (e.g., Matheron, 1971) as follows:

$$278 \quad \gamma_L(\xi) = \frac{\mu}{L^2} \int_{-L}^L (L - |x|) \left(1 - \exp\left[-\frac{|\xi + x|}{\lambda}\right]\right) dx - \frac{\mu}{L^2} \int_{-L}^L (L - |x|) \left(1 - \exp\left[-\frac{|x|}{\lambda}\right]\right) dx, \quad (18)$$

279 This results in

$$280 \quad \gamma_L(\xi) = \mu \frac{\lambda^2}{L^2} \left\{ 2 \exp\left[-\frac{|\xi|}{\lambda}\right] - \exp\left[-\frac{|\xi| + L}{\lambda}\right] - \exp\left[-\frac{|\xi| - L}{\lambda}\right] + 2\left(-1 + \exp\left[-\frac{L}{\lambda}\right] + \frac{L}{\lambda}\right) \right\} \quad |\xi| \geq L. \quad (19)$$

281 For the development of Eq. (19), the reader is referred to Appendix E.

282 Extending Eq. (19) to two dimensions and substituting it into Eq. (9), the

283 covariance functions of the random input parameters ( $f$  and  $\beta$ ) can then be expressed,

284 respectively, as

$$285 \quad C_f(\xi_1, \xi_2) = \mu_f \frac{\left(\exp\left[\frac{L}{\lambda_f}\right] - 1\right)^2}{L^2} \frac{\lambda_f - \sqrt{\xi_1^2 + \xi_2^2}}{\sqrt{\xi_1^2 + \xi_2^2}} \exp\left[-\frac{\sqrt{\xi_1^2 + \xi_2^2} + L}{\lambda_f}\right], \quad (20a)$$

$$286 \quad C_\beta(\xi_1, \xi_2) = \mu_\beta \frac{\left(\exp\left[\frac{L}{\lambda_\beta}\right] - 1\right)^2}{L^2} \frac{\lambda_\beta - \sqrt{\xi_1^2 + \xi_2^2}}{\sqrt{\xi_1^2 + \xi_2^2}} \exp\left[-\frac{\sqrt{\xi_1^2 + \xi_2^2} + L}{\lambda_\beta}\right]. \quad (20b)$$

287 Using Eq. (20) in Eq. (10), it follows that the spectral density functions of the

288 fluctuations of  $f$  and  $\beta$  each have the form

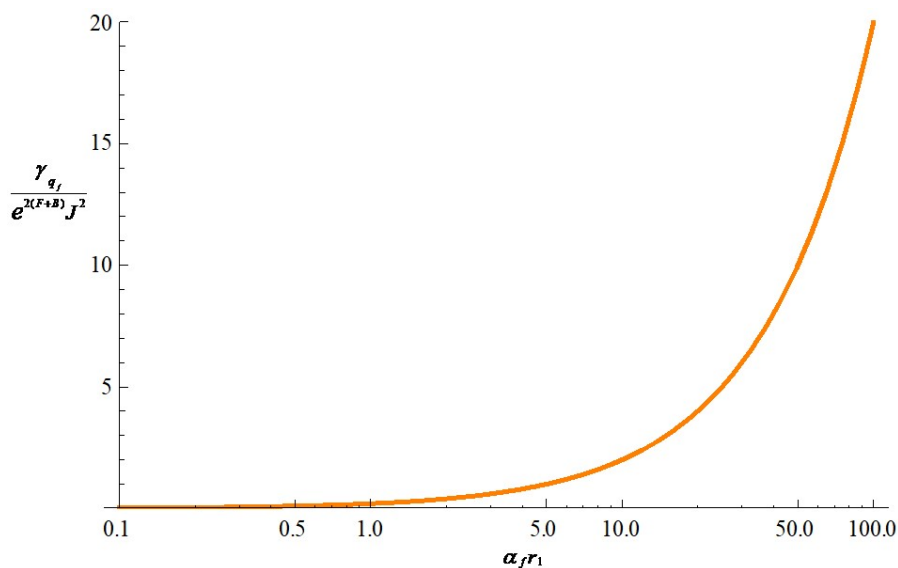
$$289 \quad S_f(w_1, w_2) = \frac{\mu_f}{2\pi} \frac{\left(\exp\left[\frac{L}{\lambda_f}\right] - 1\right)^2}{\left(\frac{L}{\lambda_f}\right)^2} \frac{\lambda_f^2 (w_1^2 + w_2^2)}{[1 + \lambda_f^2 (w_1^2 + w_2^2)]^2}, \quad (21a)$$

$$290 \quad S_\beta(w_1, w_2) = \frac{\mu_\beta}{2\pi} \frac{\left(\exp\left[\frac{L}{\lambda_\beta}\right] - 1\right)^2}{\left(\frac{L}{\lambda_\beta}\right)^2} \frac{\lambda_\beta^2 (w_1^2 + w_2^2)}{[1 + \lambda_\beta^2 (w_1^2 + w_2^2)]^2}. \quad (21b)$$

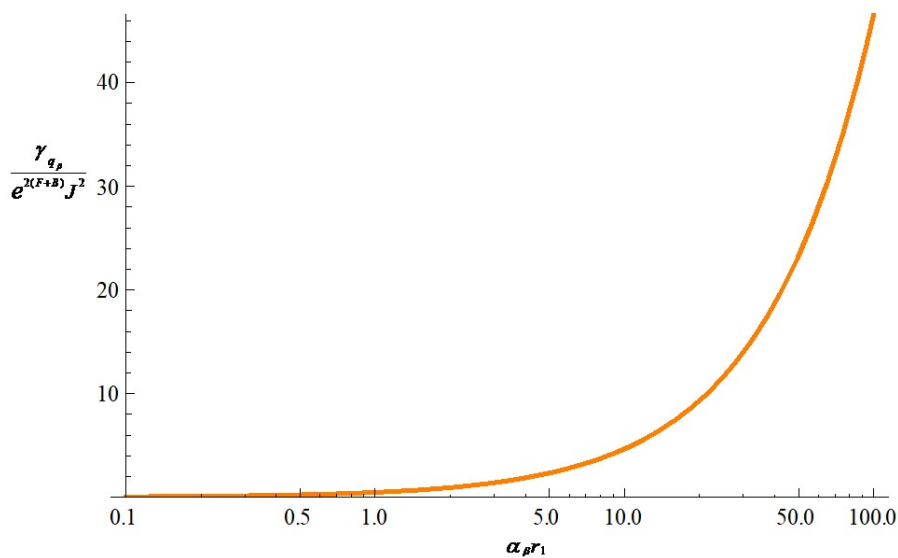
291



292 (a)



294 (b)



296 Figure 3. The components of the semivariogram of the integrated specific discharge in  
297 the mean flow direction, (a)  $\gamma_{q_f}$  reflecting the effect of variation in the log hydraulic  
298 conductivity fields, and (b)  $\gamma_{q_\beta}$  reflecting the effect of variation in the log aquifer  
299 thickness fields, as a function of parameters  $\alpha_f$  and  $\alpha_\beta$  and separation distance.



300 Finally, substituting Eq. (21) into Eqs. (7) and (8), the semivariograms of  
301 depth-averaged head and the semivariogram of integrated specific discharge in the  
302 mean flow direction can now be evaluated.

303 The practical advantage of using the general stochastic modeling framework  
304 developed here with the intrinsic hypothesis is a wider range of possible  
305 semivariogram models compared to the cases with second-order stationarity. The  
306 condition of second-order stationarity is rarely encountered in nature (e.g., Wu and Hu,  
307 2004) and is difficult to verify using the limited experimental data available. It is  
308 under these conditions that the presented stochastic approach has the greatest utility of  
309 quantification of the flow field variability.

310

## 311 **5 Conclusions**

312

313 In this work, a general stochastic methodology is developed for quantifying the  
314 variability of flow fields in heterogeneous confined aquifers of variable thickness. The  
315 stochastic theories developed here, namely the semivariograms of depth-averaged  
316 hydraulic head and integrated specific discharge used to characterize flow field  
317 variability, can address the effects of nonstationarity due to variations in parameters  
318 and output. The proposed stochastic theories generalize existing stochastic theory,



319 which applies to second order stationary random input parameters, to nonstationary  
320 random input parameters. Stationarity in the spatial variation of soil properties is very  
321 rarely encountered in nature. The stochastic theories developed here improve the  
322 quantification of flow field variability in natural confined aquifers.

323 The results show that the introduction of intrinsic random input parameters leads  
324 to a nonstationary process of depth-averaged hydraulic head fluctuations (an intrinsic  
325 random function of order 1) and a nonstationary process of integrated specific  
326 discharge fluctuations (an intrinsic random function of order 0). Application of the  
327 stochastic theories developed here to the case where the variability of a random input  
328 parameter can be characterized by a linear semivariogram model shows that larger  
329 parameters  $\alpha_f$  and  $\alpha_\beta$  increase the variability of the depth-averaged head and thus the  
330 variability of the integrated discharge in the mean flow direction.

331

### 332 **Appendix A: A steady flow through a heterogeneous confined aquifer** 333 **of variable thickness**

334

335 According to Chang et al. (2021), an essentially horizontal, steady groundwater flow  
336 through a heterogeneous confined aquifer of variable thickness can be represented as  
337 follows:



$$338 \quad \frac{\partial^2}{\partial x_i^2} \tilde{h}(x_1, x_2) + \left[ -\frac{\partial}{\partial x_i} \ln K(x_1, x_2) + 2 \frac{\partial}{\partial x_i} \ln b(x_1, x_2) \right] \frac{\partial}{\partial x_i} \tilde{h}(x_1, x_2) = 0 \quad i = 1, 2, \quad (A1)$$

339 which is the vertically integrated form of the continuity equation. In Eq. (A1),  $\tilde{h}(x_1, x_2)$   
 340 is the depth-averaged hydraulic head,  $K(x_1, x_2)$  is the hydraulic conductivity and  $b(x_1, x_2)$   
 341 is the aquifer's thickness. From Eq. (A1), it can be seen that the variations in  
 342 hydraulic conductivity and aquifer thickness that occur affect the depth-averaged  
 343 hydraulic head. If the log conductivity and log thickness in Eq. (A1) are treated as  
 344 stochastic (random) variables, Eq. (A1) can be considered as a stochastic partial  
 345 differential equation with a stochastic output  $\tilde{h}$ .

346 Similarly, integrating the equation for specific discharge along the  $x_3$ -axis and  
 347 applying Leibniz's rule leads to the vertically integrated specific discharge in the  $x_i$   
 348 direction as follows:

$$349 \quad Q_{x_i}(x_1, x_2) = -K(x_1, x_2) b(x_1, x_2) \frac{\partial}{\partial x_i} \tilde{h}(x_1, x_2) \quad (A2)$$

350 Under the influence of a uniform mean hydraulic gradient, the perturbation  
 351 equations for the depth-average hydraulic head and integrated specific discharge  
 352 associated with Eqs. (A1) and (A2) are given, respectively, by

$$353 \quad \frac{\partial^2}{\partial x_i^2} h(x_1, x_2) = J \left[ -\frac{\partial}{\partial x_1} f(x_1, x_2) + 2 \frac{\partial}{\partial x_1} \beta(x_1, x_2) \right] \quad i = 1, 2, \quad (A3)$$

$$354 \quad q_i(x_1, x_2) = e^{F+B} J \left\{ [f(x_1, x_2) + \beta(x_1, x_2)] \delta_{ii} - \frac{\partial}{\partial x_i} h(x_1, x_2) \right\} \quad i = 1, 2. \quad (A4)$$

355 In Eqs. (A3) and (A4),  $h$  and  $q_i$  are the fluctuations of depth-average head and  
 356 integrated discharge, respectively,  $J$  is the constant mean hydraulic gradient,  $F$  and  $B$



357 are the mean log conductivity and mean aquifer thickness, respectively, and  $f$  and  $\beta$   
358 are the fluctuations of log conductivity and log aquifer thickness, respectively. A  
359 detailed development of Eqs. (A3) and (A4) can be found in Chang et al. (2021).

360

## 361 **Appendix B: Derivation of Eq. (5)**

362

363 Since equation (A3) is linear, it can alternatively be divided into two parts as follows:

$$364 \quad \frac{\partial^2}{\partial x_1^2} h_f(x_1, x_2) + \frac{\partial^2}{\partial x_2^2} h_f(x_1, x_2) = J \frac{\partial}{\partial x_1} f(x_1, x_2), \quad (\text{B1a})$$

$$365 \quad \frac{\partial^2}{\partial x_1^2} h_\beta(x_1, x_2) + \frac{\partial^2}{\partial x_2^2} h_\beta(x_1, x_2) = 2J \frac{\partial}{\partial x_1} \beta(x_1, x_2). \quad (\text{B1b})$$

366 Applying Eqs. (3a) and (4b) into Eq. (B1a), it follows that

$$367 \quad \frac{\partial^2}{\partial x_1^2} A_f(x_1, x_2; w_1, w_2) + \frac{\partial^2}{\partial x_2^2} A_f(x_1, x_2; w_1, w_2) = J \frac{w_1}{\sqrt{w_1^2 + w_2^2}} \exp[i(w_1 x_1 + w_2 x_2)], \quad (\text{B2})$$

368 which is known as Poisson's equation and has a particular solution in the form

$$369 \quad A_f(x_1, x_2; w_1, w_2) = J \frac{w_1}{\sqrt{w_1^2 + w_2^2}} \frac{1 - \exp[i(w_1 x_1 + w_2 x_2)] + i(w_1 x_1 + w_2 x_2)}{w_1^2 + w_2^2}. \quad (\text{B3})$$

370 Similarly, using Eqs. (3b) and (4c), Eq. (B1b) can be written as follows:

$$371 \quad \frac{\partial^2}{\partial x_1^2} A_\beta(x_1, x_2; w_1, w_2) + \frac{\partial^2}{\partial x_2^2} A_\beta(x_1, x_2; w_1, w_2) = 2J \frac{w_1}{\sqrt{w_1^2 + w_2^2}} \exp[i(w_1 x_1 + w_2 x_2)], \quad (\text{B4})$$

372 and accordingly,



$$A_{\beta}(x_1, x_2; w_1, w_2) = 2J \frac{w_1}{\sqrt{w_1^2 + w_2^2}} \frac{1 - \exp[i(w_1 x_1 + w_2 x_2)] + i(w_1 x_1 + w_2 x_2)}{w_1^2 + w_2^2}. \quad (\text{B5})$$

374 Finally, substituting Eqs. (B4) and (B5) into Eq. (4), Eq. (5) is obtained.

375

376 **Appendix C: Expressions for the functions in Eq. (7)**

377

$$\Xi_1(\mathbf{x} - \mathbf{y}) = J^2 \int_{-\infty}^{\infty} \int_{-\infty}^{\infty} \frac{w_1^2}{(w_1^2 + w_2^2)^3} [1 - \cos(w_1 r_1) \cos(w_2 r_2) + \frac{1}{2}(w_1^2 r_1^2 + w_2^2 r_2^2)] S_{S_f}(w_1, w_2) dw_1 dw_2, \quad (\text{C1})$$

$$\Xi_2(\mathbf{x}, \mathbf{y}) = J^2 \int_{-\infty}^{\infty} \int_{-\infty}^{\infty} \frac{w_1^3}{(w_1^2 + w_2^2)^3} [-\sin(w_1 x_1) \cos(w_2 x_2) + \sin(w_1 y_1) \cos(w_2 y_2)] S_{S_f}(w_1, w_2) dw_1 dw_2, \quad (\text{C2})$$

$$\Xi_3(\mathbf{x}, \mathbf{y}) = J^2 \int_{-\infty}^{\infty} \int_{-\infty}^{\infty} \frac{w_1^2 w_2}{(w_1^2 + w_2^2)^3} [-\cos(w_1 x_1) \sin(w_2 x_2) + \cos(w_1 y_1) \sin(w_2 y_2)] S_{S_f}(w_1, w_2) dw_1 dw_2, \quad (\text{C3})$$

$$\Omega_1(\mathbf{x} - \mathbf{y}) = J^2 \int_{-\infty}^{\infty} \int_{-\infty}^{\infty} \frac{w_1^2}{(w_1^2 + w_2^2)^3} [1 - \cos(w_1 r_1) \cos(w_2 r_2) + \frac{1}{2}(w_1^2 r_1^2 + w_2^2 r_2^2)] S_{S_{\beta}}(w_1, w_2) dw_1 dw_2, \quad (\text{C4})$$

$$\Omega_2(\mathbf{x}, \mathbf{y}) = J^2 \int_{-\infty}^{\infty} \int_{-\infty}^{\infty} \frac{w_1^3}{(w_1^2 + w_2^2)^3} [-\sin(w_1 x_1) \cos(w_2 x_2) + \sin(w_1 y_1) \cos(w_2 y_2)] S_{S_{\beta}}(w_1, w_2) dw_1 dw_2, \quad (\text{C5})$$

$$\Omega_3(\mathbf{x}, \mathbf{y}) = J^2 \int_{-\infty}^{\infty} \int_{-\infty}^{\infty} \frac{w_1^2 w_2}{(w_1^2 + w_2^2)^3} [-\cos(w_1 x_1) \sin(w_2 x_2) + \cos(w_1 y_1) \sin(w_2 y_2)] S_{S_{\beta}}(w_1, w_2) dw_1 dw_2, \quad (\text{C6})$$

384  $r_1 = x_1 - y_1$ ,  $r_2 = x_2 - y_2$ , and  $S_{S_f}$  and  $S_{S_{\beta}}$  are the spectral density functions of the stationary

385 processes of  $S_f$  and  $S_{\beta}$ , respectively.





386

### 387 **Appendix D: Derivation of Eq. (13)**

388

389 The condition for Eq. (13) that the absolute value of  $\xi$  is greater than or equal to  $L$  ( $|\xi$   
390  $\geq L$ ) means that  $\xi \geq L$  or  $\xi \leq -L$ . For  $\xi \geq L$ , the integrand of the integral Eq. (13) can be  
391 expressed as

$$\begin{aligned} 392 \quad \gamma_L(\xi) &= \frac{\alpha}{L^2} \int_{-L}^0 (L+x)(|\xi|+x) dx + \frac{\alpha}{L^2} \int_0^L (L-x)(|\xi|+x) dx - \frac{\alpha}{L^2} \int_{-L}^0 (L+|x|)(-x) dx - \frac{\alpha}{L^2} \int_0^L (L-x)x dx \\ 393 \quad &= \alpha \left( |\xi| - \frac{L}{3} \right). \end{aligned} \quad (\text{D1})$$

394 For  $\xi \leq -L$ , the integrand of the integral Eq. (13) can be expressed as

$$\begin{aligned} 395 \quad \gamma_L(\xi) &= \frac{\alpha}{L^2} \int_{-L}^0 (L+x)(|\xi|-x) dx + \frac{\alpha}{L^2} \int_0^L (L-x)(|\xi|-x) dx - \frac{\alpha}{L^2} \int_{-L}^0 (L+|x|)(-x) dx - \frac{\alpha}{L^2} \int_0^L (L-x)x dx \\ 396 \quad &= \alpha \left( |\xi| - \frac{L}{3} \right). \end{aligned} \quad (\text{D2})$$

397

### 398 **Appendix E: Derivation of Eq. (19)**

399

400 Analogous to Eq. (13), the integral of Eq. (18) under the condition  $|\xi| \geq L$  can be  
401 evaluated separately as the integration of Eq. (18) under the condition  $\xi \geq L$  and that  
402 under the condition  $\xi \leq -L$ .

403 For  $\xi \geq L$ ,



$$\begin{aligned}
 404 \quad \gamma_L(\xi) &= \frac{\mu}{L^2} \int_{-L}^0 (L+x)(1 - \exp[-\frac{|\xi|+x}{\lambda}]) dx + \frac{\mu}{L^2} \int_0^L (L-x)(1 - \exp[-\frac{|\xi|+x}{\lambda}]) dx \\
 405 \quad &\quad - \frac{\mu}{L^2} \int_{-L}^0 (L+x)(1 - \exp[\frac{x}{\lambda}]) dx - \frac{\mu}{L^2} \int_0^L (L-x)(1 - \exp[-\frac{x}{\lambda}]) dx \\
 406 \quad &= \mu \frac{\lambda^2}{L^2} \left\{ 2\exp[-\frac{|\xi|}{\lambda}] - \exp[-\frac{|\xi|+L}{\lambda}] - \exp[-\frac{|\xi|-L}{\lambda}] + 2(-1 + \exp[-\frac{L}{\lambda} + \frac{L}{\lambda}]) \right\}. \quad (E1)
 \end{aligned}$$

407 For  $\xi \leq -L$ ,

$$\begin{aligned}
 408 \quad \gamma_L(\xi) &= \frac{\mu}{L^2} \int_{-L}^0 (L+x)(1 - \exp[-\frac{|\xi|-x}{\lambda}]) dx + \frac{\mu}{L^2} \int_0^L (L-x)(1 - \exp[-\frac{|\xi|-x}{\lambda}]) dx \\
 409 \quad &\quad - \frac{\mu}{L^2} \int_{-L}^0 (L+x)(1 - \exp[\frac{x}{\lambda}]) dx - \frac{\mu}{L^2} \int_0^L (L-x)(1 - \exp[-\frac{x}{\lambda}]) dx \\
 410 \quad &= \mu \frac{\lambda^2}{L^2} \left\{ 2\exp[-\frac{|\xi|}{\lambda}] - \exp[-\frac{|\xi|+L}{\lambda}] - \exp[-\frac{|\xi|-L}{\lambda}] + 2(-1 + \exp[-\frac{L}{\lambda} + \frac{L}{\lambda}]) \right\}. \quad (E2)
 \end{aligned}$$

411

412 *Data availability.* No data was used for the research described in the article.

413

414 *Author contributions.* C-MC: Conceptualization, Methodology, Formal analysis,

415 Writing - original draft preparation, Writing - review & editing.

416 C-FN: Conceptualization, Methodology, Formal analysis, Writing - original draft

417 preparation, Writing - review & editing, Supervision, Funding acquisition.

418 C-PL: Conceptualization, Methodology, Formal analysis, Writing - original draft

419 preparation, Writing - review & editing.

420 I-HL: Conceptualization, Methodology, Formal analysis, Writing - original draft

421 preparation, Writing - review & editing.

422

423 *Competing interests.* The authors declare that they have no conflict of interest.



424

425 *Acknowledgements.* Research leading to this paper has been partially supported by the  
426 grant from the Taiwan Ministry of Science and Technology under the grants MOST  
427 110-2123-M-008-001-, MOST 110-2621-M-008-003-, and MOST  
428 110-2811-M-008-533.

429

## 430 **References**

431

432 Bardossy, A.: Introduction to Geostatistics, Institute of Hydraulic Engineering,  
433 University of Stuttgart, 1997.

434 Chang, C-M, Ni, C-F, Li, W-C, Lin, C-P, and Lee, I-H: Stochastic analysis of the  
435 variability of groundwater flow fields in heterogeneous confined aquifers of  
436 variable thickness, *Stoch. Environ. Res. Risk Assess.*,  
437 <https://doi.org/10.1007/s00477-021-02125-7>, 2021.

438 Christakos, G.: *Random Field Models in Earth Sciences*, Academic, San Diego, 1992.

439 Dagan, G.: *Flow and Transport in Porous Formations*, Springer, New York, 1989.

440 Dell'Oca, A., Guadagnini, A., and Riva, M.: Interpretation of multi-scale permeability  
441 data through an information theory perspective, *Hydrol. Earth Syst. Sci.*, 24,  
442 3097-3109, 2020.



- 443 Gelhar, L.W.: Stochastic Subsurface Hydrology, Prentice Hall, Englewood Cliffs,  
444 New Jersey.
- 445 Journel, A. G. and Huijbregts, C. J.: Mining Geostatistics, Academic Press, New York,  
446 1978.
- 447 Matheron, G.: Les variables regionalisees et leur estimation, Masson, Paris, 1965.
- 448 Matheron, G.: The theory of regionalized variables and its applications, Les Cahiers  
449 du Centre de Morphologie Mathematique in Fontainebleu, Paris, 1971.
- 450 Molz, F. J., Rajaram, H., and Lu, S. L.: Stochastic fractal-based models of  
451 heterogeneity in subsurface hydrology: Origins, applications, limitations, and  
452 future research questions, Rev. Geophys., 42, RG1002, 2004.
- 453 Priestley, M. B.: Evolutionary spectra and non-stationary processes, J. R. Stat. Soc. Ser.  
454 B., 27(2), 204-237, 1965.
- 455 Rubin, Y.: Applied Stochastic Hydrogeology, Oxford University Press, New York,  
456 2003.
- 457 Usowicz, B. and Lipiec, J.: Spatial variability of saturated hydraulic conductivity and  
458 its links with other soil properties at the regional scale, Sci. Rep., 11, 1-12, 2021.
- 459 Wu, J. and Hu, B.: Stochastic study of solute flux in nonstationary flow field  
460 conditioning on measured data, Developments in Water Science, 55(1), 705-716,  
461 2004.



- 462 Yaglom, A. M.: Correlation Theory of Stationary and Related Random Functions, Vol.  
463 I: Basic Results, Springer Series in Statistics, Springer, New York, 1987.
- 464 Zhang, D.: Stochastic Methods for Flow in Porous Media: Coping with Uncertainties,  
465 Academic Press, San Diego, 2002.  
466